Supply Temperature Stabilization of Decentralized Solar Thermal Collectors for Integration into District Heating and Cooling System

Raimonds Bogdanovics[1], Aleksandrs Zajacs[1]

[1] Riga Technical University, Institute of Heat, Gas and Water Technology, Riga (Latvia)

Abstract

The solar thermal collector with return/supply connection to the district heating system through a heat exchanger with a 3-way valve for temperature control was investigated. The study of supply temperature fluctuations and stabilization possibilities in northern climatic conditions was performed by an energy simulation software package and a test facility with flat plate and vacuum thermal collectors. Here we report the experimentally discovered temperature fluctuation in different working regimes (heat carrier supply temperature 80°C, 65°C, 50°C, 30°C) and different weather conditions (sunny and cloudy), as well as analyze the potential of using solar collectors for radiative cooling during the night period and present the computer model validation results.

Keywords: solar thermal collector, district heating and cooling, control accuracy

1. Introduction

The global average temperature in 2017 was about 1°C above pre-industrial levels (as a reference point for the sampling period 1850 − 1900) and continues to increase by about 0.2°C over ten years, explained by various greenhouse gas emissions based on human activity (Allen et al., 2018). Many scientists predict severe consequences for the environment as rising ocean levels, increase frequency of droughts, reduced biodiversity, reduce agricultural land and pastures, etc. As temperatures rise, so will the number of heat-related human health problems, and the spread of dangerous diseases such as malaria, tropical fever (Hoegh-Guldberg et al., 2018).

One way to slow down climate change is to pursue a carbon-neutral policy, to which 195 countries have committed themselves by 2050 under the Paris Agreement. Greenhouse gas emissions reduction can be achieved by replacing fossil fuels (coal, oil, natural gas) with renewable energy sources (solar, wind, hydro). With the development of renewable energy technologies, their efficiency is increasing but costs are falling, so households are increasingly using them to reduce the cost of heating and hot water in buildings, as well as greenhouse gas emissions.

At the end of 2019, the installed capacity of global solar collectors was 479 GWth (684 million m^2) with a total heat production of 389 TWh per year; in 2018, 12,192 m^2 flat surface solar collectors with a total capacity of 8.5 MWth and 3240 m^2 vacuum tube solar collectors with a capacity of 2.3 MWth were installed and operated in Latvia, just as in 2019 a 21,672 m^2 flat surface solar collector park with a capacity of 15 MWth was built in Salaspils (Latvia), which was connected to the existing district heating systems of the city (Weiss and Spörk-Dür, 2020). Hybrid gas boilers in combination with solar thermal panels were promoted on the market as the most efficient and environmentally friendly solutions. Nevertheless, the annual savings for a single-family house are minor and the payback time for the installation of hybrid gas/solar systems could exceed 20 years (Borodinecs et al., 2019). Despite the long payback period of solar thermal systems in Baltic countries, the market is slowly growing, mainly due to support from the EU and other funds (Valančius et al., 2020). Also, a high potential of renewable energy sources can be spotted for mobile solutions. The use of renewable energy for heat and ventilation in the mobile unit was investigated in the study (Bogdanovics et al., 2021) and solutions described in this study can be adopted for mobile use in the future.

Previous studies (Zajacs et al., 2020) confirmed that solar collectors produce the largest amount of heat energy in summer, when the solar intensity is the highest, while the heat demand during summer is the lowest because heat

doi:10.18086/eurosun.2022.11.02 Available at http://proceedings.ises.org

is only used to prepare hot water. During the day, hot water consumption fluctuates significantly, leading to a mismatch between heat supply and demand. This problem is partially solved by using hot water storage tanks, but if the tank volume is too small, or the household does not use hot water for a long time, solar collectors have nowhere to return heat energy, and the system temperature starts to rise and stagnation and overheating may occur. It has been found (Hillerns, 2001) that the propylene glycol-water mixture ages prematurely under the influence of high temperatures, which manifests itself as a darkening of the liquid and a decrease in the pH value, so in solar collectors, under conditions of constant stagnation, irreversible degradation of the heat carrier occurs within $2-3$ weeks. As a result of the oxidation reaction, the glycol liquid decomposes chemically, forming acidic organic compounds (lactic acid, oxalic acid, acetic acid, formic acid) as reaction products.

Almost all methods of overheating protection of solar collectors are aimed at preventing solar collectors from generating heat in the event of excess heat, thus reducing the total amount and efficiency of heat produced. If solar collectors are connected to a sufficiently large district heating network (Brange et al., 2016; Heymann et al., 2017; Lennermo et al., 2019), then the problem of stagnation could be solved without reducing the efficiency of the system, as district heating provides hot water preparation and supplies heat to factories for production processes also during the summer. Solar collectors installed in households in the summer months usually produce more heat than required, so creating a heat supply system where unused heat can be diverted to a district heating system would not only improve the overall efficiency of the system but also provide financial benefits and reduce the payback time of solar collectors.

Integrating large solar parks into a district heating system has been studied extensively (Paulick et al., 2018; Sørensen et al., 2012; Winterscheid et al., 2017). Large solar parks are mainly integrated into the district heating system, but there is very little information on small, decentralized solutions when household roof solar panels are connected to district heating networks. If energy is both consumed and produced within the household, such households are called “prosumers” or “proactive consumers”. Currently, this concept is already successfully used in the electricity market, but the concept can also be used in the field of heat energy (Brange et al., 2016).

Low heat carrier temperatures allow to significantly increase the efficiency of solar thermal collectors (Lund et al., 2021). In Strasbourg (France), the initial cost of solar collectors in the fourth-generation (annual average temperature regime 55/25°C) is reduced by 30% compared to the third-generation (80/45°C) heating system, because to achieve this the amount of heat energy per year requires a smaller solar collector area due to higher solar collector efficiency, with the percentage difference increasing in regions with the lowest solar radiation intensity (Averfalk and Werner, 2020).

Compared to the fourth-generation, the concept of the fifth-generation system includes even lower heat carrier temperatures ($20-40$°C) and the possibility to use heating networks simultaneously as a source of heat and cold for heating and cooling buildings using heat pumps. The concept of “proactive consumers” is one of the components of the fifth-generation district heating system. In total, there are at least 40 fifth-generation district heating systems in operation in Europe (mainly in Germany and Switzerland) and some of them have integrated solar systems (Buffa et al., 2019; Millar et al., 2021; Revesz et al., 2020).

In fifth-generation district heating and cooling system, radiative cooling technology – heat is radiated to outer space through a transparency window in the atmosphere between 8 and 13 μm (Bartoli et al., 1977) – can be used to produce cooling energy by solar colectors. The theoretical calculation with ZnS cover-based vacuum solar collectors shows about 75 W/m^2 cooling power at night with 5 °C difference between ambient air and absorber temperatures (Ao et al., 2021). The experimental study shows maximum net cooling power of 96 W/m^2 at night and 45 W/m^2 at noon under an average of 952 W/m^2 solar radiation (Zhao et al., 2019). As the night radiative cooling is more efficient, it is beneficial to produce heat during the day and cool during the night.

In this study, the solar thermal collector with return/supply connection to the district heating through a heat exchanger with a 3-way valve for temperature control was investigated. The study of supply temperature fluctuations and stabilization possibilities in northern climatic conditions was performed by the TRNSYS energy simulation software package and a test facility with flat plate and vacuum thermal collectors, that was placed on the university roof in Riga, Latvia. Here we report the experimentally discovered temperature fluctuation in different working regimes and different weather conditions and the computer model validation results.

2. Methods

2.1. Test facility

The test facility with flat plate and vacuum thermal collectors was created and placed on the Riga Technical University roof in Riga, Latvia, providing the location of solar collectors to the south without shading. Test facility is composed of 4 modules (see Figure 2):

- M1: parallel-connected flat plate and vacuum tube solar collectors with separate circulation pumps;
- M2: solar collector connection module for district heating system;
- M3: district heating system simulated with electric water heater;
- M4: thermal energy consumer simulated with variable speed water heating unit.

The test facility is compact and mobile (see Figure 1). Collectors slope 45°. Pipes, pumps, valves and controls are located in a water-resistant cabinet with a key. The heating unit is above the cabinet and is protected from rain. To avoid overheating, it is possible to mechanically cover collectors. Management is possible both on-site and remotely via an Internet connection. Equipment requires an electricity connection. The rig is intended to be operated at an outdoor temperature above 0°C, but for safety purposes, a water-glycol mixture (50%) is used as a heat carrier.

Fig. 1: Test facility

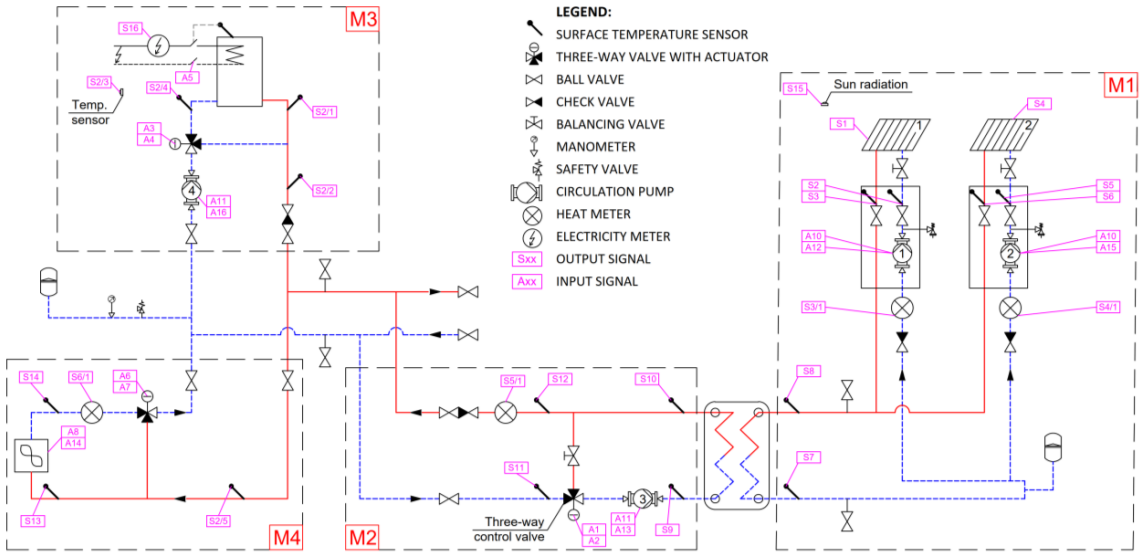

Fig. 2: Test facility schematic

The 3-way valve (see M2 in Figure 2) control speed may be changed in the range 20% − 500%, changing the time of providing a signal for opening/closing the valve (run time) and the waiting time between two consecutive opening/closing signals (see Figure 3). Three control speeds were investigated: low (20%), normal (100%), fast (500%).

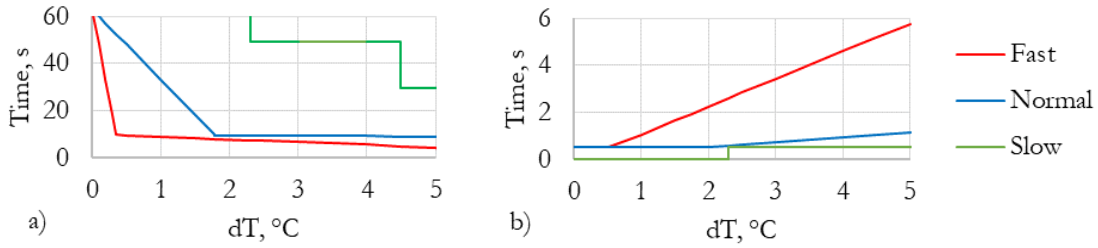

Fig. 3: Control signal (a) waiting time and (b) run time depending on the temperature difference (dT) between actual and specified heat carrier supply temperature

The experiment took place during the summer weather. Measurement step: 2.0 s. Data were filtered so only measurements then heat carrier from module M2 were injected into M4 (see Figure 2) are taken into account. Data were grouped in a way that each hour can be analyzed separately.

Hourly average solar radiation with standard deviation [W/m^2], as well as hourly average heat carrier supply temperature with standard deviation [°C], were calculated. If hourly solar radiation SD < 100 W/m^2, it is assumed that during this hour the weather was sunny, otherwise – cloudy.

During the experiment, four temperature regimes (T1/T2) for the summer period were used:

- HighT: 80/50°C, regime usually used in the big scale 3rd district heating systems;
- MediumT: 65/42°C, regime usually used in the small-scale 3rd district heating systems;
- LowT: 50/30°C, regime represent 4th generation district heating;
- UltraLowT: 30/15°C, regime represent 5th generation district heating.

Legend for cases:

- 80 / 65 / 50 / 35 - required supply temperature, °C;
- L / N / F – low / normal / fast control speed (see Figure 3);
- S / C – sunny / cloudy hour.

All temperature regimes were performed both in sunny and cloudy weather conditions and with three different 3-way valve control speeds (see Figure 3).

2.2. Computer model

The computer model (see Figure 4) was developed by TRNSYS 18 energy simulation software package. It represents the M1 and M2 modules from Figure 2. Data about M3 and M4 modules are implemented by input values based on the test facility measured values.

Input data: ambient air temperature, return heat carrier temperature and solar intensity [W/m^2] during the day based on the experiment measurement data (step 2.0 s), values between input data are linearly interpolated. Solar position from Meteonorm database for a specific day in Riga (Latvia). Pressure in the district heating system fluctuates; supply pipe 60±6 kPa, return pipe: 33±5 kPa.

Simulation time: one day from 7:00 till 19:00. Simulation step 0.1 s.

Assumptions: no specific data about wind speed, so Meteonorm database data is used; in the model heat carrier flow speed is not considered, so model response time might be faster.

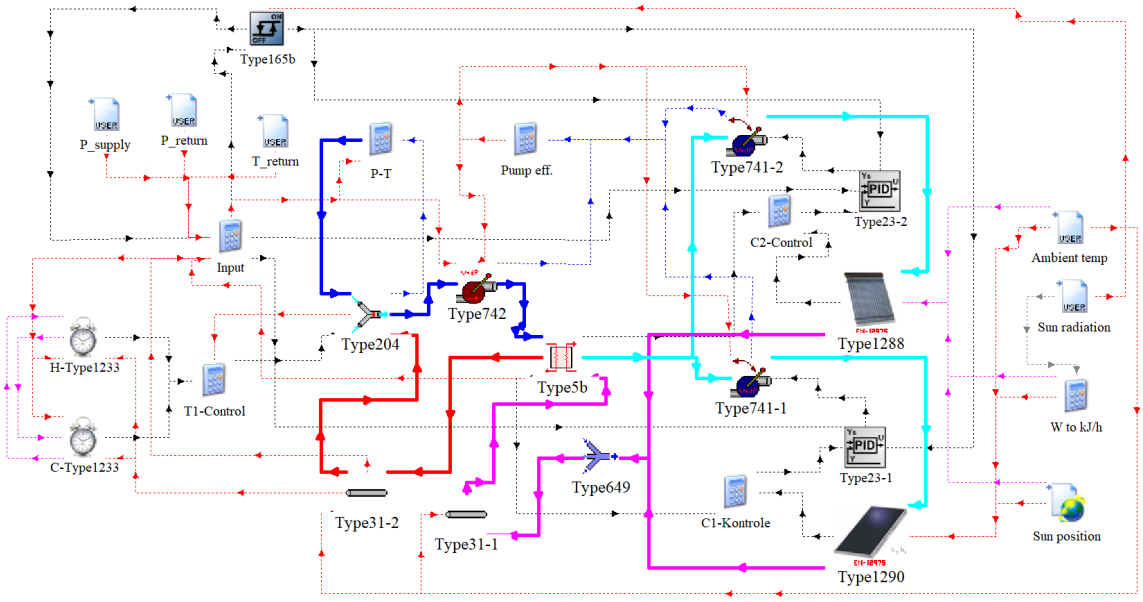

Fig. 4: Computer model created with the TRNSYS energy simulation software package

Main component parameters:

- Three-way valve with actuator (Type204). Time constant: 15 s; hysteresis: 5%; curve: linear / linear;
- Control signal (H-Type1233 and C-Type1233). The program according to Figure 3;
- Flat plate solar collector (Type1290). Area (total): 2.03 m^2; efficiency: 0.712; coefficient α_1: 3.18 W/m^2K; coefficient α_2: 0.010 W/m^2K^2; heat capacity: 6.3 kJ/m2K; slope: 45°; direction: to equator;
- Vacuum tube solar collectors (Type1288). Area (total): 1.95 m^2; efficiency: 0.362; coefficient α_1: 0.60 W/m^2K; coefficient α_2: 0.005 W/m^2K^2; heat capacity: 6.5 kJ/m^2K; slope: 45°; direction: to equator;
- Circulation pump (Type742). Pressure 42.7 kPa, efficiency 3-19% (depending on flow);
- Circulation pump (Type741). Pressure 30.0 kPa; max flow: 100 kg/h; efficiency 3-19%;
- PID controller (Type23). Gain constant: 3; integral time: 1 s; derivative time: 4 s;
- Heat exchanger (Type5b): heat transfer coefficient 425 W/K;
- Pipes with defined heat losses (Type-31). The actual loss of heat in the system is not known, therefore, for the model, heat losses are assumed to be equivalent to heat losses in DN15 (1/2'') insulated steel tube with a heat loss factor of 10 W/m^2K. The total assumed equivalent pipe length is 14 m.

3. Results

3.1. Heat carrier temperature fluctuations

For each temperature regime, average supply temperature, measurement standard deviation, kurtosis and skewness were calculated. It was found that the shape of the probability distribution plot of the heat carrier temperature deviation from desired supply temperature (see Figure 5) usually has two peaks – near 0 and some degrees Celsius behind. For instance, case 50-F-C with average temperature deviation ATD = -0.49°C, standard deviation SD = 1.11 °C, kurtosis K = 0.65 and skewness S = 0.17 or 80-L-S with ATD = -0.65 °C, SD = 2.66°C, K = 0.42, S = -0.63 has potential for control improvement. Only few cases have the ideal desired distribution characteristics like 50-N-S with ATD = 0.32°C, SD = 0.89°C, K = 21.78, S = -3.67.

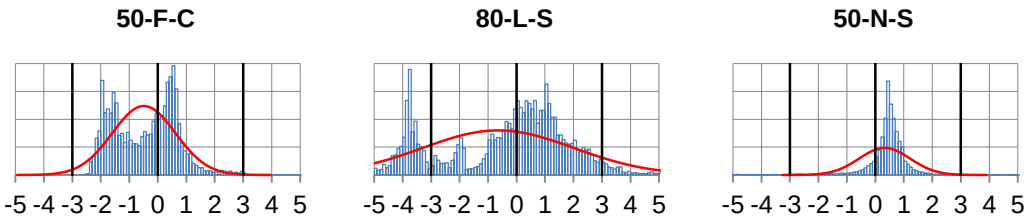

Fig. 5: Measured heat carrier supply temperature distribution; x-axis: supply temperature deviation from required temperature; y-axis: amount of measured supply temperatures; red line – normal distribution

Results show that temperature fluctuations cannot be perfectly described with normal distribution plot, but anyway, standard deviation parameter can be used to compare cases to find out the scope of temperature fluctuations (see Figure 6). The greater is the standard deviation (SD), the greater temperature fluctuates. The greatest SD = 2.85°C is found in the combination 80-L-C. The smallest SD = 0.89°C is found in the case 50-N-S. In most cases, SD in cloudy weather is greater than in sunny weather.

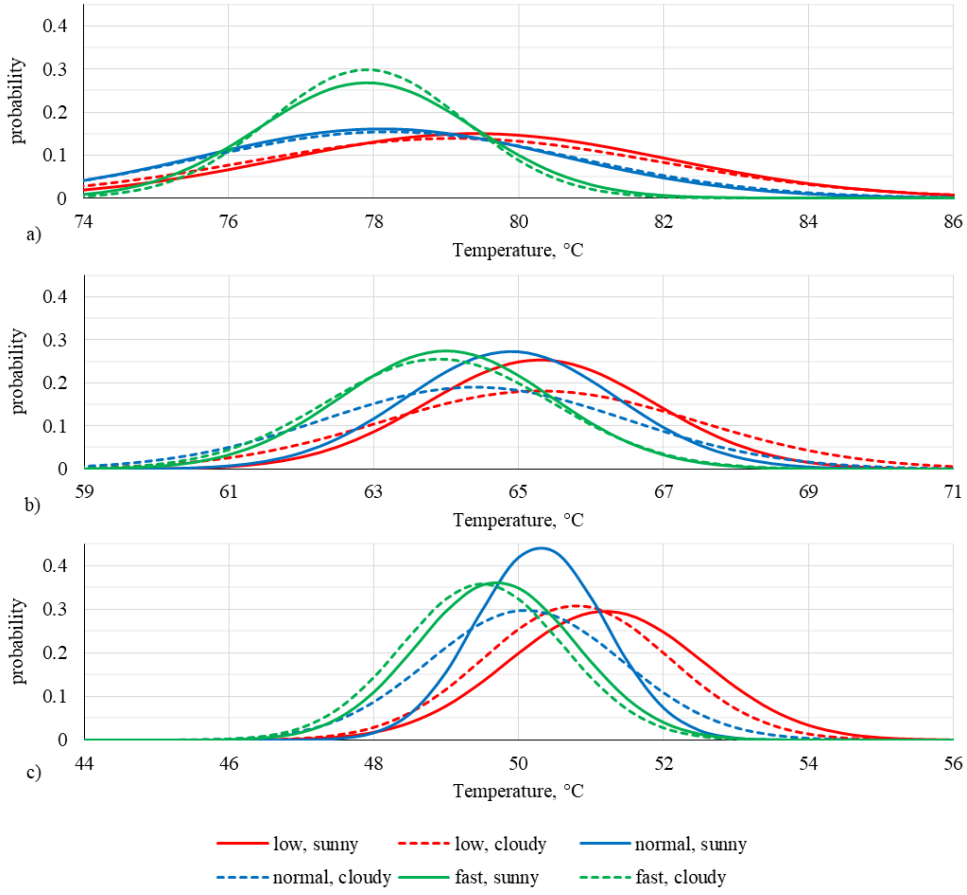

Fig. 6: Supply temperature normal distribution plots, (a) HighT: 80/50°C, (b) MediumT: 65/42°C, (c) LowT: 50/30°C

Based on the temperature regime, ranges of average temperature deviation (ATD) and standard deviation (SD):

- HighT: ATD = -2.07 – -0.65°C; SD = 1.34 – 2.85°C;
- MediumT: ATD = -1.07 – 0.34°C; SD = 1.46 – 2.19°C;
- LowT: ATD = -0.49 – 1.23°C; SD = 0.89 – 1.34°C;
- UltraLowT: ATD = -0.47 – 0.40°C; SD = 1.15 – 1.51°C.

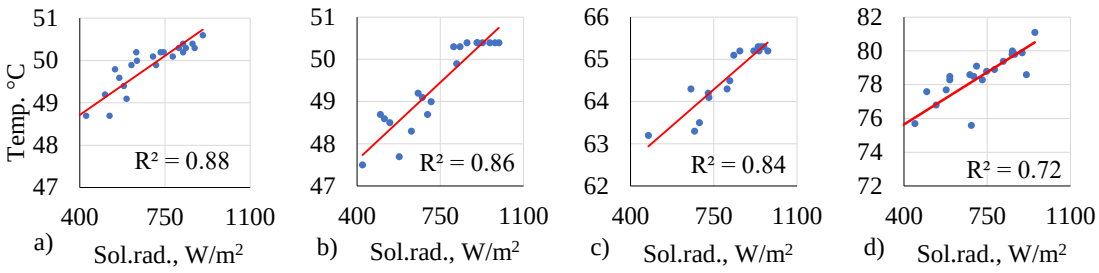

Fig. 7: Hourly average supply temperature [°C] dependence on hourly average solar radiation [W/m2], (a) 50-N-C, (b) 50-F-S, (c) 65-N-S, (d) 80-L-C

It is found (see Figure 7) that in all cases the hourly average supply temperature is lower at the lower solar radiation level and the relation between these two parameters is strong ($p < 0.05$).

3.2. Computer model validation results

Computer simulations were performed for 18 days (6 days per one temperature regime, 6 days per one control program in all possible combinations). The simulated supply temperature results were analyzed in the same way as experimentally measured data. The standard deviation of supply temperature from the experiment was compared (see Figure 8) with the standard deviation of supply temperature from the simulation based on the same weather conditions, temperature regime and control program.

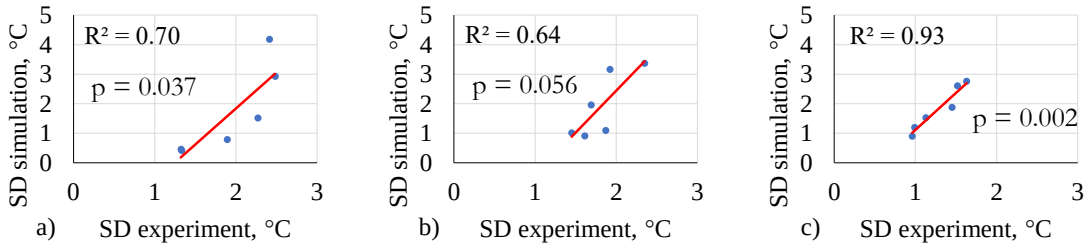

Fig. 8: Standard deviation [°C] based on experimental measurements compared to simulation results, (a) HighT: 80/50°C, (b) MediumT: 65/42°C, (c) LowT: 50/30°C

The linear regression analysis shows that there is a strong relation between experimental and simulation SD, so it is possible to use the computer model to analyze different components' impact on temperature fluctuations.

The difference between the experimental and simulation SD might be explained by assumptions and simplifications of the model that results in faster response time and higher average heat carrier temperature in the model compared to the measured temperature. The main cause might be in the simplification of the hydraulic model: no precise hydraulic resistance and geometry of facility components are used in the model as well as heat carrier flow speed is not considered. To increase the model accuracy, more measurements in different regimes should be done and more sensors, including pressure sensors, should be used.

3.3. Heating energy production

The produced energy amount from 7:00 till 19:00 was measured and simulated for 2 days – 16.08.2022 (cloudy day) and 28.08.2022 (sunny day) for MediumT (65/42°C) regime for both solar collectors. Results show that the simulated energy amount from collectors (without heat losses in pipes and system components) is 60-108% higher than measured (see Figure 9) which can be explained by high heat losses at the test facility compared to system size, so in small solar collector systems, the component proper insulation is very important.

Sunny day vacuum collector produced 2.63 kWh, flat plate collector 4.01 kWh; operation time: 10:30 – 17:30. Cloudy day vacuum collector produced 1.91 kWh, flat plate collector 2.66 kWh; operation time: 10:30 – 16:20.

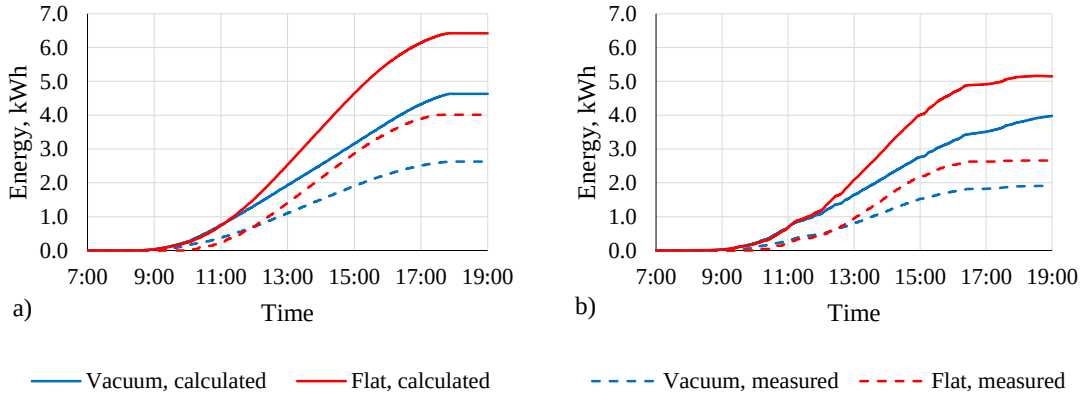

Fig. 9: Cumulative energy production, calculated and measured values, (a) sunny day, (b) cloudy day

3.4. Cooling energy production

The solar collector radiative cooling potential was investigated on 2 clear sky nights from 00:00 till 6:00.

Tab. 1: Measured values from the test facility during the night operation

Day	04.08.2022		07.08.2022	
Solar collector type	Vacuum	Flat plate	Vacuum	Flat plate
Average T to solar collector, °C	36.9	36.7	18.4	18.4
Average T from solar collector, °C	35.2	33.6	17.9	17.3
Average flow through solar collector, l/h	53.9	55.6	50.4	48.8
Average cooling power, $W/m^2_{total\ area}$	45	89	11	27
Produced cooling energy, Wh	543	1037	128	311
Average ambient air temperature, °C	19.6	19.6	14.7	14.7

Results show (see Table 1) that the cooling potential of flat plate solar collector is 2 times higher compared to vacuum tube solar collector and with higher heat carrier temperature the cooling power increase can be explained by increasing transmission heat loss. During the experiment, the heat carrier temperature was above ambient air temperature and the temperature drop in collectors was not significant.

4. Conclusion

Within this study the test facility and the TRNSYS 18 computer model were developed with the purpose to simulate and measure the performance of two types of solar collectors (vacuum tube and flat plate) in different working regimes and how they perform as a prosumer unit for thermal energy feed into the district heating network. The main desired parameter was constant supply temperature from the solar collectors' system to the district heating system. The computer model was validated within three temperature regimes and correlation coefficients for each regime were determined.

It is found that there is a difference in average supply temperature and temperature fluctuations depending on weather conditions, heat carrier temperature regime, and three-way valve control speed, achieving the best performance in sunny weather with the lower required supply temperature. With increasing the speed of the control valve, the standard deviation of heat carrier temperature fluctuations mainly decreases but the average temperature decreases too. The shape of the probability distribution plot of the heat carrier temperature deviation from desired supply temperature does not represent the normal distribution plot and usually has two peaks.

The measured produced energy demand is significantly lower than the simulated which might be explained by significant heat losses in the test facility, so additional investigations and further improvements of the test facility and computer model are going to be done in future research.

5. Acknowledgments

This work has been supported by the European Social Fund within the Project No 8.2.2.0/20/I/008 «Strengthening of PhD students and academic personnel of Riga Technical University and BA School of Business and Finance in the strategic fields of specialization» of the Specific Objective 8.2.2 «To Strengthen Academic Staff of Higher Education Institutions in Strategic Specialization Areas» of the Operational Programme «Growth and Employment». This publication was supported by Riga Technical University's Doctoral Grant programme.

6. References

Allen, M.R., Dube, O.P., Solecki, W., Aragón-Durand, F., Cramer, W., Humphreys, S., Kainuma, M., Kala, J., Mahowald, N., Mulugetta, Y., Perez, R., Wairiu, M., Zickfeld, K., 2018. Chapter 1. Framing and Context, in: Global Warming of 1.5°C. An IPCC Special Report on the Impacts of Global Warming of 1.5°C above Pre-Industrial Levels and Related Global Greenhouse Gas Emission Pathways, in the Context of Strengthening the Global Response to the Threat of Climate Change.

Ao, X., Liu, J., Hu, M., Zhao, B., Pei, G., 2021. A rigid spectral selective cover for integrated solar heating and radiative sky cooling system. Sol. Energy Mater. Sol. Cells 230, 111270. https://doi.org/10.1016/j.solmat.2021.111270

Averfalk, H., Werner, S., 2020. Economic benefits of fourth generation district heating. Energy 193, 116727. https://doi.org/10.1016/j.energy.2019.116727

Bartoli, B., Catalanotti, S., Coluzzi, B., Cuomo, V., Silvestrini, V., Troise, G., 1977. Nocturnal and diurnal performances of selective radiators. Appl. Energy 3, 267–286. https://doi.org/10.1016/0306-2619(77)90015-0

Bogdanovics, R., Borodinecs, A., Zemitis, J., Zajacs, A., 2021. Using a mobile modular energy unit with PV panels for heating. ASHRAE J. 63, 38–46.

Borodinecs, A., Bogdanovics, R., Prozuments, A., Tihana, J., Gaujena, B., 2019. Evaluation of hybrid heating systems with a combination of fossil and renewable energy sources, in: IOP Conference Series: Earth and Environmental Science. https://doi.org/10.1088/1755-1315/297/1/012050

Brange, L., Englund, J., Lauenburg, P., 2016. Prosumers in district heating networks - A Swedish case study. Appl. Energy 164. https://doi.org/10.1016/j.apenergy.2015.12.020

Buffa, S., Cozzini, M., D'Antoni, M., Baratieri, M., Fedrizzi, R., 2019. 5th generation district heating and cooling systems: A review of existing cases in Europe. Renew. Sustain. Energy Rev. 104, 504–522. https://doi.org/10.1016/j.rser.2018.12.059

Heymann, M., Rühling, K., Felsmann, C., 2017. Integration of Solar Thermal Systems into District Heating - DH System Simulation. Energy Procedia 116, 394–402. https://doi.org/10.1016/j.egypro.2017.05.086

Hillerns, F., 2001. The behaviour of heat transfer media in solar active thermal systems in view of the stagnation conditions, in: IEA-SHC Task 26 Industry Workshop. Borlänge, Sweden.

Hoegh-Guldberg, O., Jacob, D., Taylor, M., Bindi, M., Brown, S., Camilloni, I., Diedhiou, A., Djalante, R., Ebi, K.L., Engelbrecht, F., Guiot, J., Hijioka, Y., Mehrotra, S., Payne, A., Seneviratne, S.I., Thomas, A., Warren, R., Zhou, G., 2018. Chapter 3. Impacts of 1.5ºC Global Warming on Natural and Human Systems, in: Global Warming of 1.5°C. An IPCC Special Report on the Impacts of Global Warming of 1.5°C above Pre-Industrial Levels and Related Global Greenhouse Gas Emission Pathways, in the Context of Strengthening the Global Response to the Threat of Climate Change. pp. 175–311.

Lennermo, G., Lauenburg, P., Werner, S., 2019. Control of decentralised solar district heating. Sol. Energy 179, 307–315. https://doi.org/10.1016/j.solener.2018.12.080

Lund, H., Østergaard, P.A., Nielsen, T.B., Werner, S., Thorsen, J.E., Gudmundsson, O., Arabkoohsar, A., Mathiesen, B.V., 2021. Perspectives on fourth and fifth generation district heating. Energy 227, 120520.

https://doi.org/10.1016/j.energy.2021.120520

Millar, M.A., Yu, Z., Burnside, N., Jones, G., Elrick, B., 2021. Identification of key performance indicators and complimentary load profiles for 5th generation district energy networks. Appl. Energy 291, 116672. https://doi.org/10.1016/j.apenergy.2021.116672

Paulick, S., Schroth, C., Guddusch, S., Rühling, K., 2018. Resulting Effects on Decentralized Feed-In into District Heating Networks - A Simulation Study. Energy Procedia 149, 49–58. https://doi.org/10.1016/j.egypro.2018.08.168

Revesz, A., Jones, P., Dunham, C., Davies, G., Marques, C., Matabuena, R., Scott, J., Maidment, G., 2020. Developing novel 5th generation district energy networks. Energy 201, 117389. https://doi.org/10.1016/j.energy.2020.117389

Sørensen, P.A., Nielsen, J.E., Battisti, R., Schmidt, T., Trier, D., 2012. Solar district heating guidelines: Collection of fact sheets. WP3 – D3.1 & D3.2. Sol. Distric Heat. 152.

Valančius, R., Jurelionis, A., Jonynas, R., Borodinecs, A., Kalamees, T., Fokaides, P., 2020. Growth rate of solar thermal systems in Baltic States: Slow but steady wins the race? Energy Sources, Part B Econ. Planning, Policy 15, 423–435.

Weiss, W., Spörk-Dür, M., 2020. Solar Heat Worldwide. Global market development and trends in 2019.

Winterscheid, C., Dalenback, J.-O., Holler, S., 2017. Integration of solar thermal systems in existing district heating systems. Energy 137, 579–585.

Zajacs, A., Borodiņecs, A., Neviero, I., 2020. Optimal use of solar collectors in small-scale districts. IOP Conf. Ser. Mater. Sci. Eng. 869. https://doi.org/10.1088/1757-899X/869/4/042039

Zhao, D., Aili, A., Zhai, Y., Lu, J., Kidd, D., Tan, G., Yin, X., Yang, R., 2019. Subambient Cooling of Water: Toward Real-World Applications of Daytime Radiative Cooling. Joule 3, 111–123. https://doi.org/10.1016/j.joule.2018.10.006